soil systems

MDPI

Article

Lowland Integrated Crop–Livestock Systems with Grass Crops Increases Pore Connectivity and Permeability, Without Requiring Soil Tillage

Jordano Vaz Ambus [1], Amanda Romeiro Alves [1], Douglas Leandro Scheid [1], Antonio Celso Dantas Antonino [2] and José Miguel Reichert [1,2,*]

[1] Soils Department, Universidade Federal de Santa Maria, Santa Maria 97105-900, Brazil; jordano.ambus@acad.ufsm.br (J.V.A.); amanda.romeiro@acad.ufsm.br (A.R.A.); douglas.scheid@ufsm.br (D.L.S.)
[2] Department of Nuclear Energy, Universidade Federal de Pernambuco, Recife 50740-545, Brazil; antonio.antonino@ufpe.br
* Correspondence: reichert@ufsm.br

Abstract: Enhancing integrated crop–livestock systems (ICLSs) to improve land-use efficiency is a critical goal. Understanding the ICLS impacts on lowland soils is key to sustainable agricultural practices. Our objective was to test whether adopting ICLSs in lowlands improves soil structure, pore connectivity, and water and air permeability. This study was conducted in a long-term field trial, consisting of the following production systems with flood-irrigation rice: rice–fallow–rice, under conventional tillage and absence of grazing (RFR-ct); rice-grazed ryegrass–rice, under no-tillage and grazing (RGrR-nt); rice-grazed ryegrass–soybean-grazed ryegrass–rice, under no-tillage and grazing (RGrS/RGrR-nt); and a grazed pasture-consortium (winter) and succession field (summer), with no-till rice every 4 years (P4R-nt). Core samples were collected after grazing (October 2018), harvesting (March 2019), and grazing (October 2019). We analyzed soil air permeability, saturated hydraulic conductivity, pore connectivity by computed tomography. Soil tillage in a semi-direct system generated discontinuous porosity. Systems with intense trampling or less surface protection are affected by shearing on topsoil, reducing pore continuity. ICLSs are mainly composed of ryegrass–rice mitigated the harmful effects of trampling, and improved soil structure and functioning. Systems without soil tillage exhibited higher pore connectivity and pores with vertical orientation. Finally, soil tillage is not required to improve structural quality in ICLSs.

Keywords: soil structure; roots; grazing; tomography; pore continuity

Citation: Ambus, J.V.; Alves, A.R.; Scheid, D.L.; Antonino, A.C.D.; Reichert, J.M. Lowland Integrated Crop–Livestock Systems with Grass Crops Increases Pore Connectivity and Permeability, Without Requiring Soil Tillage. *Soil Syst.* **2024**, *8*, 111. https://doi.org/10.3390/soilsystems8040111

Academic Editor: Sören Thiele-Bruhn

Received: 26 July 2024
Revised: 15 October 2024
Accepted: 23 October 2024
Published: 30 October 2024

1. Introduction

Integrated crop–livestock systems (ICLSs) increase production diversity and are key to sustainable agricultural development [1,2]. The role of agriculture as a source of food for populations around the world is indisputable. While meeting the growing demand for food is crucial, cropping systems must operate efficiently to prevent the depletion of natural resources [3].

Brazilian subtropic ICLSs are based on grain-crop cultivation in summer, such as soybeans (*Glycine max*), corn (*Zea mays*), and rice (*Oryza sativa*), and pastures for animal consumption in winter [4]. The introduction of winter pastures in lowland areas with hydromorphic soils, which are predominantly used in rice monoculture in southern Brazil [5], is a promising alternative in terms of land-use diversification and efficiency [6]. However, the consequences of adopting this cropping system on soil structure in lowlands remain largely unknown.

Soil serves as a key indicator of the overall quality of cropping system management. Soil structure, encompassing aggregation and porosity, plays a pivotal role in governing the

internal matrix dynamics. Soil structure influences critical aspects of plant development, such as water supply and nutrients, and provides necessary physical conditions for root and microorganism development [7,8]. Porous system functioning properties are dynamic and management-sensitive; thus, they express soil heterogeneity and complexity in cropping systems [9,10]. The soil's saturated hydraulic conductivity and air permeability are a function of structural quality, especially of the pore system, dependent on pore number, connectivity, and tortuosity [11].

Lowland soils tend to hold water content above field capacity for long periods, which hinders the movement of gasses within the soil [12]. High soil moisture hinders the development of crops deprived of physiological mechanisms to compensate for oxygen absence, unlike rice, which is adapted to these conditions [13]. Moreover, soil's ability to conduct water through soil pores, which enables rapid drainage after rains or floods, is a major factor in reducing hydric stress due to excess water [14]. Therefore, the success of a crop rotation system and the establishment of pastures in lowland soils depends on a management system capable of constructing an interconnected and functional porosity.

Soil porous system dynamics can be evaluated by X-ray computed tomography (CT), which enables the generation of parameters and three-dimensional images [11,15]. This approach allows for establishing relationships between functionality properties and tomographic parameters, such as pore volume, shape, orientation and connectivity, and studying the influence of different cropping systems on pore properties [16,17].

Management significantly changes the functionality of soil pores through soil inversion during tillage [18] or compaction generated by agricultural machinery traffic or trampling by farm animals [19,20]. Conversely, cropping systems focused on soil structure conservation, cover crops use, and root development can create a favorable structural environment and improve soil health [21–25].

The ICLS are clear examples of cropping systems that, if well managed, can improve soil quality by promoting crop rotation and introducing pastures with intense root development [26]. However, the effects of ICLS on soil pore quality and functioning in lowland cropping systems under tropical conditions remain unclear. We hypothesized that implementing ICLS in lowlands, on soil initially dedicated to rice cultivation, enhances soil structure and pore functionality. The objective was to test whether adopting ICLS in lowlands improves soil structure, pore connectivity, and water and air permeability.

2. Materials and Methods

2.1. Experimental Site

The study was conducted at the Corticeiras farm, a research station of integrated crop–livestock systems in Cristal-RS, located in southern Brazil (30°58′21.4 S, 51°57′01.4 W, 28 m above sea level in altitude). The region has a humid subtropical climate (Cfa), with average annual temperatures and rainfall of 18.3 °C and 1522 mm, respectively [27]. The studied soil is a Gleyic Luvic Planosol [28] or Planossolo Háplico Eutrófico típico [29] on a flat and gently undulating terrain with a maximum slope of 4%. This soil has 17% clay, 35% silt and 48% sand (loam texture), and exhibits limited drainage capacity.

The experiment evaluated four different agricultural cropping systems and was implemented in 2013 in a complete randomized block design with three repetitions. The experimental plots, totaling 12, varied in size from 0.9 to 1.5 hectares. The studied cropping systems were as follows:

1. RFR-ct: Rice–Fallow–Rice, with tillage composed of harrowing after harvesting, here referred to as conventional tillage, without animal grazing, and the fallow period is defined by the presence of spontaneous vegetation and rice crop residues.
2. RGrR-nt: Rice–Grazed ryegrass (*Lolium multiflorum*)–Rice, consisting of growing no-till (nt) rice in summer, and ryegrass grazed in winter.
3. RGrS/RGrR-nt: Rice–Grazed ryegrass–Soybeans (*Glycine max*)–Grazed ryegrass–Rice, where rice and soybeans are cultivated in summer, alternately rotated under no-till (nt), and ryegrass grazed in winter.

4. P4R-nt: Pasture during four seasons–Rice, where birdsfoot trefoil (*Lotus corniculatus* L.) + ryegrass + white clover (*Trifolium repens*) are cultivated in winter, and a succession field composed of native pasture species naturally grows during summer. Grazing occurs during winter and summer, and no-till (NT) irrigated rice is cultivated every four years.

The experimental site has a history of rice cultivation with fallow periods that began in 1960. In 2013, the area was prepared for the experimental implantation by tilling soil and incorporating dolomitic lime (4.5 Mg ha^{-1}) in the 0–20 cm layer. Since then, the cropping systems have been carried out without soil tillage, except for RFR-ct. In these cropping systems without soil tillage, only the restoration of the water contention structures (to allow flooding within the cultivation areas) before rice growing was performed.

During the winter grazing season in RGrR-nt, RGrS/RGrR-nt, and P4R-nt, castrated male steers weighing 200 kg were introduced once the grass had reached a height of 15 cm. The continuous grazing method was used with varying stocking rates, with three animals per plot, and regulatory animals were introduced to maintain the pasture height. The pasture height was monitored every 15 days using a sward stick. Winter grazing lasted approximately four months, from June–July to October–November, depending on the cultivation sequence. For summer grazing in P4R-nt, castrated male steers aged 15 months weighing 300 kg were introduced.

Every 4 years, a cycle ends in the crop rotation system in the experiment, i.e., at that time irrigated rice is planned to be grown in all systems. Therefore, for this study, the experiment was approaching the midpoint of 2nd cycle of the cropping systems (Table 1). Annually, mineral fertilizers were applied to grain and pasture crops during the winter/summer to provide the required N, P, and K contents. The amount of fertilizer was determined based on soil analysis and technical recommendations for each crop. The complete fertilization history, as well as the planting, harvesting and grazing times in each cropping system, can be found in [30,31].

Table 1. The chronological sequence (2017–2020) of the studied integrated systems of agricultural production, highlighting the seasons when the samplings were carried out.

Acronym	2017		2018		2019		2020	
	Winter	Summer	Winter	Summer	Winter	Summer	Winter	Summer
RFR-ct	fallow	rice	fallow	rice	fallow	rice	fallow	rice
RGrR-nt	ryegrass	rice	ryegrass	rice	ryegrass	rice	ryegrass	rice
RGrS/RGrR-nt	ryegrass	soybeans	ryegrass	rice	ryegrass	soybeans	ryegrass	rice
P4R-nt	ryegrass + white clover + birdsfoot trefoil	succession field	ryegrass + white clover + birdsfoot trefoil	succession field	ryegrass + white clover + birdsfoot trefoil	succession field	ryegrass + white clover + birdsfoot trefoil	rice

2.2. Soil Sampling

The soil was sampled three times, which involved grazing in October 2018, the harvesting of summer crops in March 2019, and grazing in October 2019, to evaluate the soil's physical properties and porous system using X-ray computed tomography. In each experimental unit, soil core samples were randomly taken from topsoil (0.0–0.10 m) and subsurface (0.10–0.20 m). For soil air permeability (Ka) and saturated hydraulic conductivity (Ks) analyses, 216 core samples (4 cropping systems × 2 soil layers × 3 field replicates × 3 sampling seasons × 3 sampling replicates) were collected using polyvinyl chloride (PVC) tubes with a 0.10 m height and 0.10 m diameter. For the X-ray computed tomography analysis, we collected 72 core samples (4 cropping systems × 2 soil layers × 3 field replicates × 3 sampling seasons × 1 sampling replicate) using PVC tubes with 0.18 m height and 0.075 m diameter.

In the initial sampling in October 2018, soil organic matter content in the 0–0.10 m layer was as follows: 16 g kg^{-1} in the RFR-ct, 27 g kg^{-1} in the RGrR-nt, 28 g kg^{-1} in the RGrS/RGrR-nt, and 28 g kg^{-1} in the P4R-nt.

2.3. Soil Physical Properties

Core soil samples (0.10 m height and 0.10 m diameter) were capillary saturated for 48 h. Subsequently, the samples were brought to equilibrium at matric potentials (Ψm) of −1, −6, and −10 kPa in a sand column [32] for the determination of K_a for each Ψm, and finally, they were re-saturated for K_s determination. Soil K_a (μm^2) was determined with the aid of a constant-head permeameter, in which air flows through the soil sample at constant, low-pressure gradient (0.1 kPa) to avoid turbulent flow [33]. The K_a was calculated using Equation (1):

$$K_a = K_l \frac{\eta}{\rho_l g} \quad (1)$$

where K_l is the air conductivity (cm s^{-1}), η is the air viscosity (g s^{-1} cm^{-1}), ρ_l is the air density (g cm^{-3}), and g is the gravity acceleration (981 cm s^{-2}).

Soil K_s (mm h^{-1}) was calculated based on the flow of water flowing through the soil sample, under the application of a constant hydraulic head of 8 cm, up to a dynamic equilibrium condition, in a constant load permeameter, as described by [34]. K_s was calculated by the Darcy equation.

2.4. Porosity by X-Ray Computed Tomography (CT)

The X-ray scanning of soil core samples (0.18 m height and 0.075 m diameter) was carried out using a XTH225 ST Nikon tomograph. During this process, we used a copper filter (0.25 mm) to reduce noise effects and applied an emission power of 300 μA and 170 kV voltage. Samples were scanned in three segments of 0.06 m height, with a resolution of 40 μm. The total scanning time was approximately 4 h per sample. The CT images were reconstructed using the CT Pro 3D software (Version XT 5.1.4.3, Nikon Metrology, Brighton, MI, USA). The images were also optimized using the noise reduction presets within CT Pro 3D before being exported as 8-bit images.

For image segmentation and analysis, the software "VG Studio MAX 2.2 dongle license" was used. The image processing involved an initial step where we separated the soil volume to be analyzed. This process excluded ring walls and soil near core edges to prevent border effects on both soil structure and grayscale. As a result, a sample approximately 0.05 m in diameter and 0.06 m in height was obtained (Figure 1a,b).

The image segmentation was fundamentally based on the distinct level of X-ray attenuation exhibited by each material [35], represented by a grayscale histogram [36–39]. Three primary phases, i.e., solids, pores, and the particulate organic material of the soil sample were considered. The boundaries (grayscale) for each material of interest, referred to as "regions of interest" (ROI), were manually selected in each sample using VG Studio tools. We initially defined the area of interest containing the mineral material using the "Advanced surface determination" tool. In this process, we used the "define material by example area" function to manually select the mineral material and the background in the CT images. The "Advanced surface determination" tool in VG Studio gives an accurate determination of the structure of the selected material by locally refining the material's surface based on the gradient of gray values in the image [40]. Essentially, the algorithm adjusts the boundaries of the chosen material by considering the changes in gray values around each point. It reinterprets the same gray value according to the gray value of neighboring voxels [40].

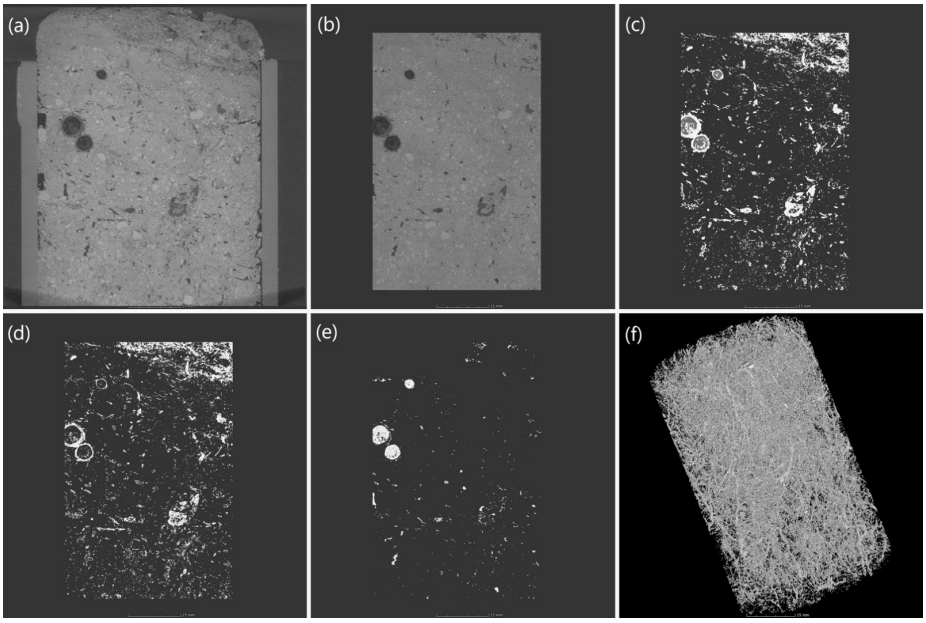

Figure 1. Steps of tomographic analysis: (**a**) scanned volume; (**b**) effective volume analyzed; (**c**) porosity and organic material, (**d**) organic material; (**e**) porosity and (**f**) 3D porosity. Sample with approximately 50 mm in diameter and 60 mm in height.

Once the boundaries of each phase were defined, we extracted the volume of the ROI most central for the study, specifically porosity (as shown in Figure 1c). From volume fractions, the surface areas of pores and organic material were quantified with "surface determination tool" that separates clusters of voxels (3D pixels), allowing for the extraction of various essential information, including volume, surface area, number of voxels, and more.

Resolved porosity (P) (cm^3 cm^{-3}) was calculated by dividing the total volume of extracted pores by the total sample volume. Connected porosity (Cp) (cm^3 cm^{-3}) was considered the volume of pores belonging to clusters larger than 1 mm^3, where Cp is the relationship between sum of these clusters and total volume of the sample. Based on the relationship between Cp and P, a connectivity index (Ci) was calculated that informs how much of P is occupied by pores greater than 1 mm^3.

An indicator that denotes connectivity between soil pores, especially over long distances, is the Γ indicator, which measures the probability that two random voxels belong to the same cluster. The indicator ranges from 0 to 1, where for the former there are many unconnected clusters, and for the latter all pore voxels belong to a single connected cluster [41]. The Γ indicator is calculated based on the transition of many disconnected clusters to a very large cluster (percolation), according to the second statistical moment of [42], and the proportion of cell pairs (distinct or not) that are connected between all pairs of permeable cells, as follows:

$$\Gamma(p) = \frac{1}{n_p^2} \sum_{i=1}^{N(X_p)} n_i^2, \quad (2)$$

where n_p is the number of all pore voxels p, X_p is the number of all clusters, and n_i is the number of pore voxels in cluster i.

2.5. Statistical Analysis

Data were initially tested for normal distribution (Shapiro–Wilk test) and homogeneity of variance (Bartlett test). As measurements were repeated over time in the same plot (within-subject factor) and cropping systems and soil depths (between-subject factors) were used, we employed a mixed model ANOVA with one within-subject factor (sampling season) and two between-subject factors (cropping system and soil depth).

Significant F-values were used to assess main effects of sampling seasons, different cropping systems, and interaction between sampling season and cropping system, as well as cropping system and soil depth effects on soil properties. The Bonferroni test was used for these comparisons. A 5% significance level was considered, and all tests were carried out using R [43].

3. Results

3.1. Soil Physical Properties

Soil saturated hydraulic conductivity (K_s) (Figure 2) did not differ among cropping systems in any soil layer. Mean K_s values were 14, 89, and 20 mm h^{-1} in topsoil, and 52, 49, and 130 mm h^{-1} in subsurface, respectively, for Grazing 2018, Harvest 2019, and Grazing 2019. Only RGrS/RGrR-nt showed variation among sampling seasons in topsoil, with K_s for Grazing 2018 (6 mm h^{-1}) and Grazing 2019 (13 mm h^{-1}) being lower compared with Harvest 2019 (95 mm h^{-1}). In P4R-nt, K_s varied among sampling seasons in subsurface, showing a decrease in K_s over time. Regarding soil layers, there was a significant difference in P4R-nt for Grazing 2018, in which K_s was higher in subsurface. In Harvest 2019, RGrR-nt had the highest K_s in topsoil, while in the subsurface layer, soil K_s was higher in the RFR-ct during Grazing 2019.

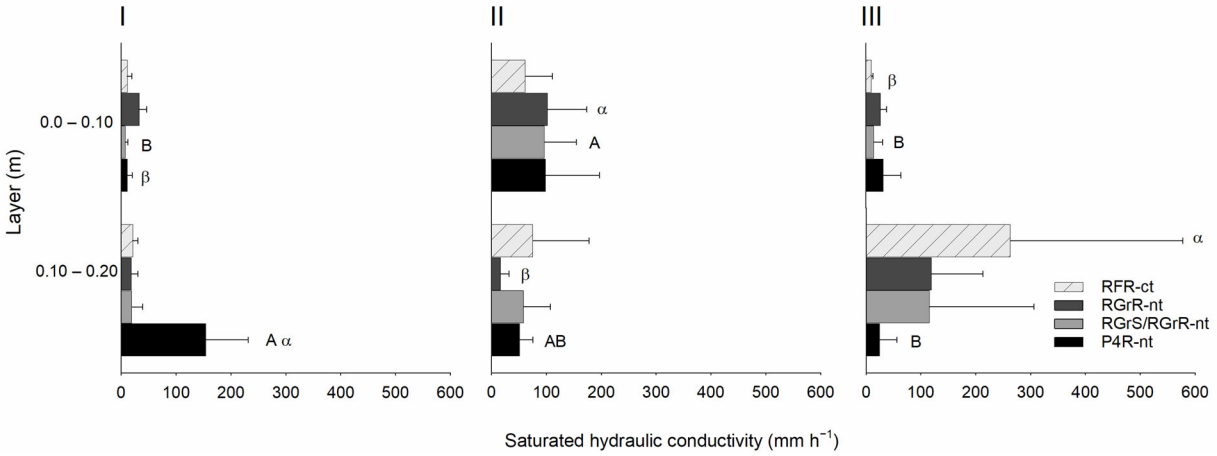

Figure 2. Soil saturated hydraulic conductivity for Grazing 2018 (**I**), Harvest 2019 (**II**), and Grazing 2019 (**III**) for two layers in four management systems. Means followed by lowercase letters (comparing cropping systems), uppercase letters (comparing sampling seasons) and Greek letters (comparing soil layers) differ by the Bonferroni test ($\alpha = 0.05$) and, when the letters do not appear, there is no significant difference. Error bars represent the standard deviation, n = 3.

Soil air permeability (Figure 3) in all evaluated matric potentials (Ψm) did not vary among cropping systems in any of the evaluated layers, and there was also no significant difference between evaluated layers for any of the cropping systems. The only difference observed corresponds to P4R-nt in topsoil for Ψm −1 kPa, in which air permeability reduced from Harvest 2019 to Grazing 2019, and Grazing 2018 did not differ from the others. In addition, air permeability increased as the soil dried, as expected.

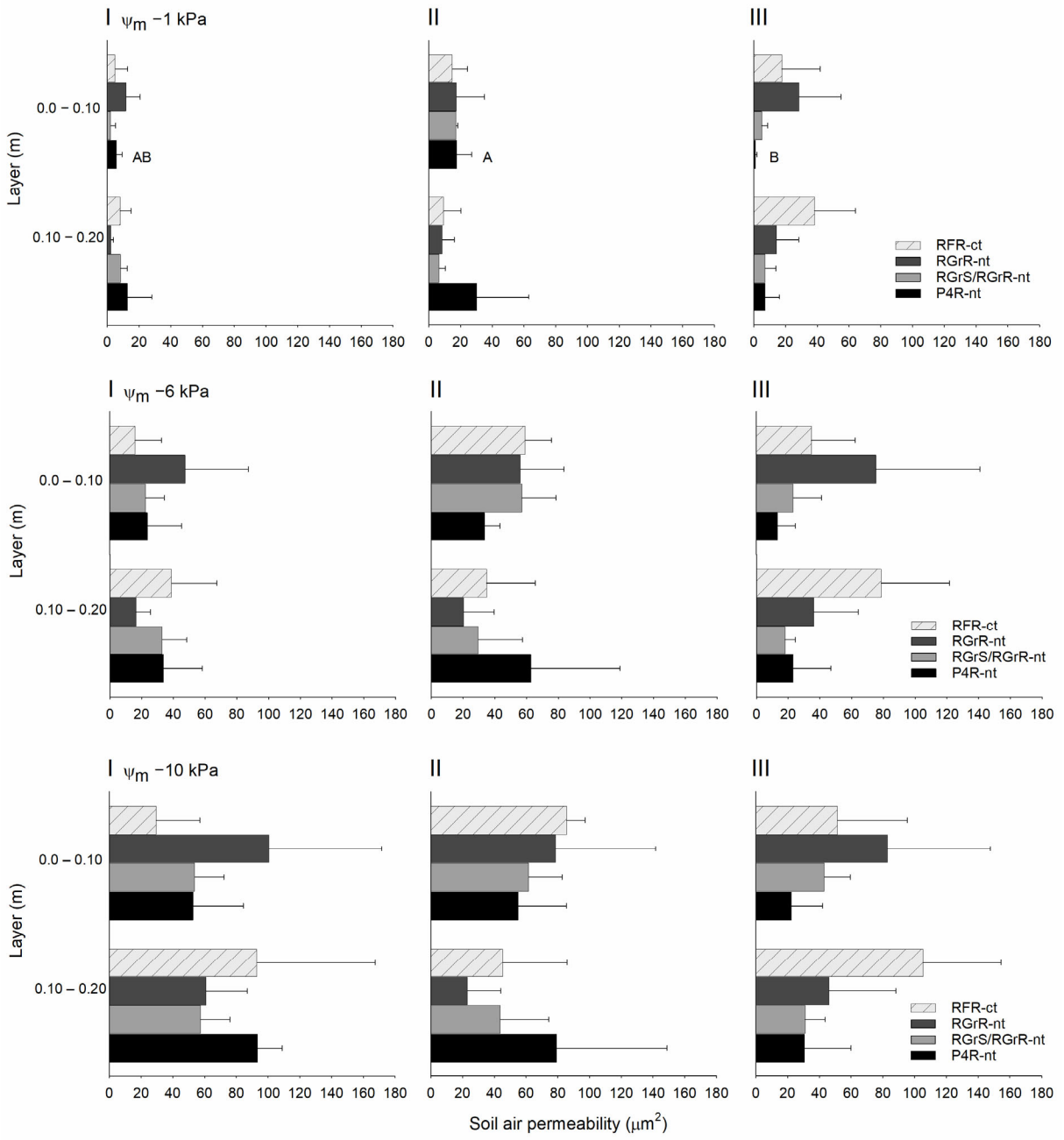

Figure 3. Soil air permeability (Ψm −1, −6 and −10 kPa) Grazing 2018 (**I**), Harvest 2019 (**II**), and Grazing 2019 (**III**) for two layers in four management systems. Means followed by lowercase letters (comparing cropping systems), uppercase letters (comparing sampling seasons) and Greek letters (comparing soil layers) differ by the Bonferroni test (α = 0.05) and, when the letters do not appear, there is no significant difference. Error bars represent the standard deviation, n = 3.

3.2. Soil Porosity by Tomography

Connected soil porosity (Figure 4) varied significantly among cropping systems only in topsoil for Grazing 2018, in which connectivity in RFR-ct and RGrR-nt was greater than in RGrS/RGrR-nt, while P4R-nt did not differ from other cropping systems. Regarding sampling seasons, in topsoil, almost all cropping systems show a reduction in connected porosity from Grazing 2018 and Harvest 2019 to Grazing 2019, and the highest connected porosity in grazed systems is observed for Harvest 2019, mainly in RGrS/RGrR-nt and P4R-nt. Considering soil layers, there was a significant difference for the two 1st seasons, in RFR-ct and RGrR-nt for Grazing 2018 and RGrR-nt, RGrS/RGrR-nt and P4R-nt for Harvest

2019, where topsoil had a greater volume of connected pores. For Grazing 2019, there was no significant difference between layers.

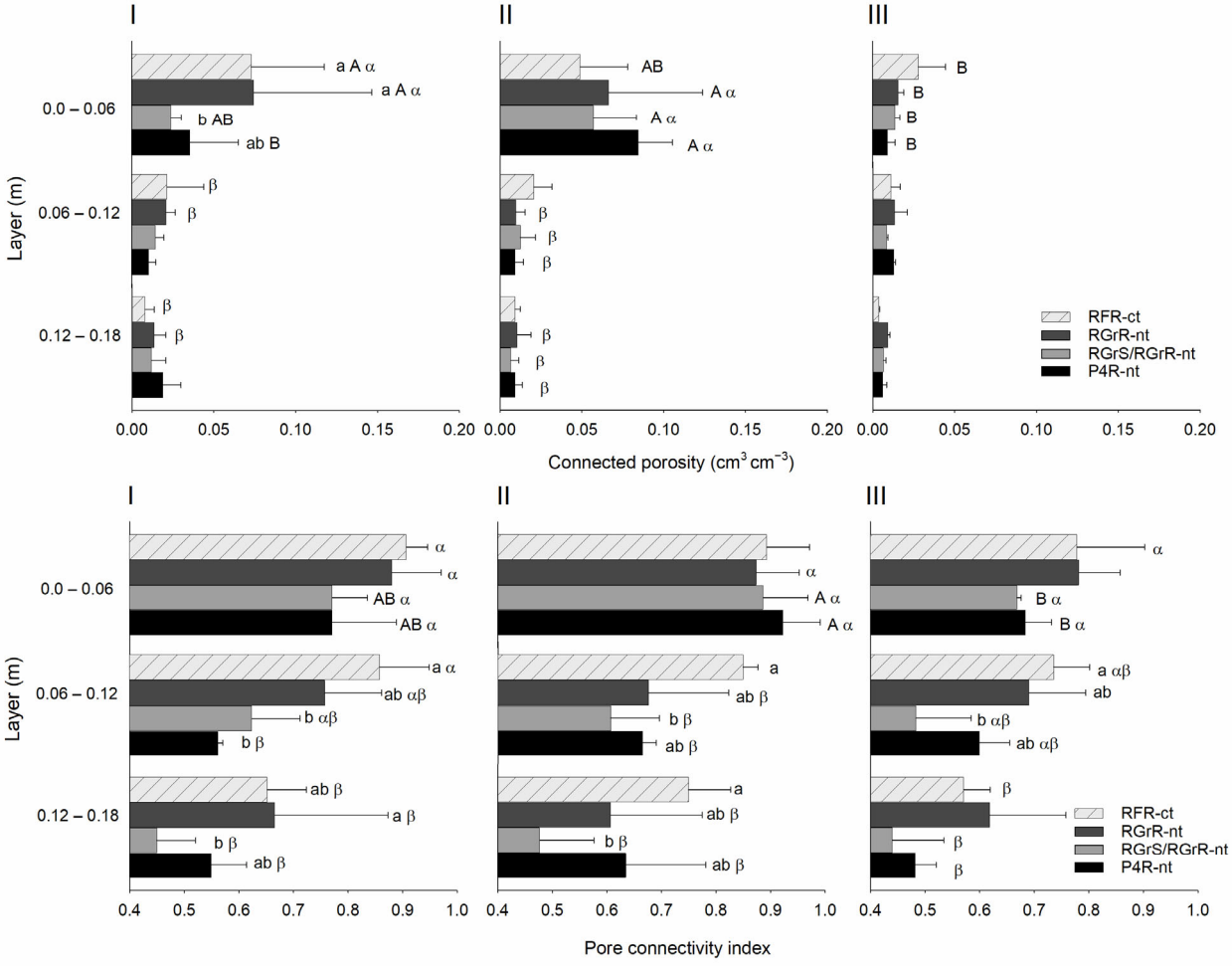

Figure 4. Connected porosity and pore connectivity index for Grazing 2018 (**I**), Harvest 2019 (**II**), and Grazing 2019 (**III**) for three layers in four management systems. Means followed by lowercase letters (comparing cropping systems), uppercase letters (comparing sampling seasons) and Greek letters (comparing soil layers) differ by the Bonferroni test ($\alpha = 0.05$) and, when the letters do not appear, there is no significant difference. Error bars represent the standard deviation, n = 3.

The pore connectivity index (Figure 4) varied among cropping systems only in the two deepest soil layers. In the 0.06–0.12 m layer, RFR-ct showed a greater pore connectivity index compared to RGrS/RGrR-nt and P4R-nt for Grazing 2018, while RGrR-nt did not differ from others. For Harvest 2019 and Grazing 2019, the RFR-ct had a greater pore connectivity index than RGrS/RGrR-nt; other cropping systems did not differ in the last two seasons. In the 0.12–0.18 m layer, RGrR-nt exhibited higher connectivity than RGrS/RGrR-nt for Grazing 2018, while RFR-ct and P4R-nt did not differ from others. For Harvest 2019, the RFR-ct had a significantly higher pore connectivity index than RGrS/RGrR-nt, with no significant differences observed among the other cropping systems, while all systems behaved similarly in the last season (Grazing 2019). Regarding sampling seasons, there was a significant difference only in topsoil and for RGrS/RGrR-nt and P4R-nt, where Harvest 2019 had higher pore connectivity than Grazing 2019, with Grazing 2018 not differing from others. There was a tendency for pore connectivity to decrease with increasing depth.

The Γ indicator (Figure 5) showed no significant differences among cropping systems at any layer or season. However, differences were observed among sampling seasons only in topsoil, with a general reduction in Γ over time. Regarding soil layers, differences were

observed in the 1st two seasons, where there is a tendency to reduce the Γ indicator from the surface to the deeper layers, especially in cropping systems with animal grazing. In Grazing 2019, there was no significant difference among soil layers.

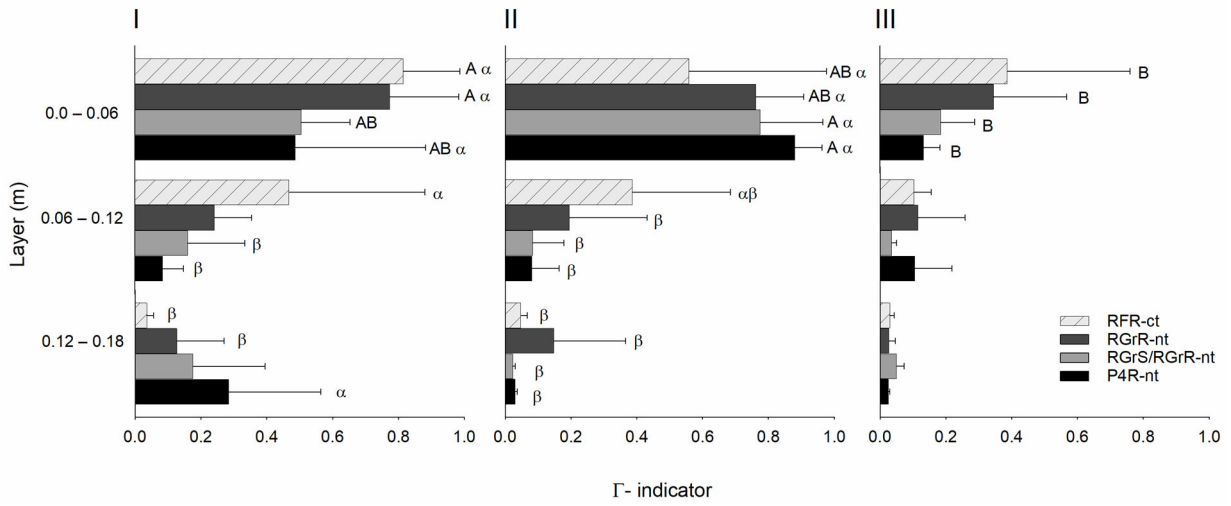

Figure 5. Γ indicator for Grazing 2018 (**I**), Harvest 2019 (**II**), and Grazing 2019 (**III**) for three layers in four management systems. Means followed by lowercase letters (comparing cropping systems), uppercase letters (comparing sampling seasons) and Greek letters (comparing soil layers) differ by the Bonferroni test (α = 0.05) and, when the letters do not appear, there is no significant difference. Error bars represent the standard deviation, n = 3.

4. Discussion

4.1. Hydraulic Conductivity and Air Permeability

Soil saturated hydraulic conductivity (K_s) did not differ among cropping systems. This outcome does not mean the cropping systems do not influence soil water movement. Although different management practices can produce similar results, it is important to consider the reasons behind the variations in soil properties. The surface layer can be thought of as the "epidermis" of soil; therefore, it is the first to experience the impacts of management. For instance, animal trampling and tillage can degrade pore structure and reduce water flow in topsoil [44,45].

Soil K_s is strongly dependent on pore quantity and quality. In conventional tillage, pore continuity is frequently disrupted by tillage operations. Moreover, the breakdown of aggregates during plowing results in denser particle accommodation, leading to reduced porosity in the short- to medium-term [46]. In grazed cropping systems, animal trampling can cause soil compaction, especially in topsoil, due to the loads applied by animal hooves [10,47,48]. Trampling also shears the soil surface, disrupting pore continuity [49], which results in a laminar soil structure.

Soil porosity, as affected by tillage, can be perceived by lower K_s in the topsoil of RFR-ct. Periodical tillage causes the breakdown of pore continuity, hampering pore functioning. The average K_s values (9.66–60.26 mm h^{-1}) observed in the management system with soil tillage (RFR-ct) were much lower than the values (383 mm h^{-1}) reported in other studies [50] in conventional tillage systems in lowlands under similar climate conditions. Nevertheless, [50] obtained much lower K_s values (1.8 mm h^{-1}) in no-till systems, compared to the average values of 31.75–101.17 mm h^{-1} observed here for integrated systems (RGrR-nt). Chiseling the soil in lowlands can temporarily increase K_s and K_a values. However, crops such as soybeans can still experience oxygen deficiency due to fluctuations in soil water levels after rainfall events [50].

Trampling also alters pore structure by compression. Thus, K_s values were reduced over time in topsoil RGrS/RGrR-nt and subsurface P4R-nt, indicating that both cropping systems experience a more intense effect of animal trampling. RGrS/RGrR-nt was culti-

vated with soybeans during the summer season, and this crop produces lower shoot and root biomass. In addition, the chemical composition of organic material from a leguminous crop, such as soybeans, has a lower C/N ratio than grasses, which accelerates leguminous decomposition [51]. Soybeans also have axial root systems with larger diameter roots and less capacity to develop in dense soils than grasses [52].

Since P4R-nt is continuously grazed, soil porosity is negatively affected by compaction, leading to reduced conductivity. In grazed cropping systems, intense root development when the soil is cultivated with forage can contribute to pore obstruction, decreasing the available space for water and solute translocation [53]. Roots also contribute to particle packing through wetting–drying cycles and the release of transient organic compounds into the rhizosphere. Loam texture soils, such as in this study, tend to have a smaller volume of macropores [54], where small changes in larger pores may reduce water conductivity. In our study, the main change was for the continuous grazing and soybean system, which can be mitigated with an adjustment and/or reduction in animal load in these cropping systems.

Cropping systems without overturning (inversion tillage) and with pasture introduction generally preserve soil structure with more continuous, connected porosity because of the absence of soil tillage, cover management, and the contribution of organic material from roots [23,55]. Although K_s did not vary among cropping systems, integrated systems are considered superior to conventional monocropping and tilled soil in terms of sustainability and productivity [1,2]. The absence of differences among cropping systems for a key soil property, such as water flow, suggests that tillage did not improve soil structure compared with grazed cropping systems, and thus tillage is not necessary.

Air permeability (K_a) is another important property when evaluating soil structural quality. We determined K_a at different water potentials to explore the relationship of soil water retention with gas movement, in addition to being a property closely linked to pore connectivity [56,57]. For a matric potential of −1 kPa (wet soil), soil K_a is considerably smaller than in drier soil because most pores are filled with water, thus reducing the free space for air flow [12].

A possible negative effect of animal trampling is the reduction in air permeability over time for continuous grazing P4R-nt for the −1 kPa water potential, since it is a management that does not have great alteration throughout the seasons. Nevertheless, this significant effect was observed for conditions of lower soil moisture or lower matrix potential, especially at −10 kPa water potential, which is frequently referred to as field capacity [58] and aeration capacity. We highlight that lowland soils are essentially hydromorphic with impaired drainage [59], which possibly contributes to soil saturation rather than to field capacity conditions.

Despite having similarities in management, grazed cropping systems differ in porous system functionality. Integrated crop–livestock systems can result in topsoil compaction, reduction in pore space, and, consequently, hamper pore functionality. Strategies to mitigate the harmful effects of animal trampling include stocking control [4,60], the cultivation of forage with high shoot-root biomass production to absorb and dissipate pressure applied by grazing animals [61], and the reduction of animal walking during grazing [62]. In our study, all the tested cropping systems had the same animal stocking during the winter season, but P4R-nt is grazed continuously in winter and summer. Thus, load accumulation affects porosity regardless of vegetation cover [48].

The cropping systems cultivated only with grass species have greater resistance to compaction because of their high biomass production and residues rich in recalcitrant compounds, with slow decomposition and the intense development of fine roots. Roots are an important soil structuring factor, as they generate pore spaces after decomposition and reduce compaction by creating biopores [55,63]. The production of root exudates influences positively edaphic biota [64], and roots from annual crops that develop in one season are decomposed in the next season, leaving highly connected voids capable of assisting in gas movement [21,25] that serve as a path for new root growth [65].

Even the no-tilled soil with animal trampling maintained its ability to conduct air, which demonstrates that grazing was not a detrimental factor to topsoil and subsurface soil structure. Loads applied to topsoil by trampling in grazed cropping systems are minimally transmitted in depth because of the attenuation/dissipation generated by organic material on the soil surface [61,66]. This leads to less disturbance in topsoil, as the magnitude of applied loads is the main factor responsible for load transmission to deeper soil layers [67]. Hence, soil cover is as important as soil organic matter for soil resistance to compaction, especially in sandy-textured soils [68]. In addition, soil organic matter is essential for soil recovery after stress, as organic matter increases soil elasticity [9,69].

Even in tilled soil, there is little disturbance in the subsurface, where soil benefits from organic material incorporated during tillage inversion [70]. Less disturbance in depth is also evident for soil water fluxes, where cropping systems had slightly higher values in deeper layers, with less influence from trampling and inversion tillage. Deeper soil layers are more protected from the negative effects of management, but are also farther away from positive effects, e.g., RGrR-nt, which had the highest K_s in the topsoil 2019 harvest. This behavior possibly results from higher root concentration in rice crops [71] and is driven by the lower natural porosity of loam-texture soils [54].

4.2. Soil Pore Connectivity and Continuity

Water and air permeability in this study exhibit diverse behaviors among soil properties that express structural quality represented by pore continuity and connectivity. The complexity of soil functionality properties allows for the use of different strategies to evaluate pore–function dynamics. Computed tomography (CT) enables studying the effect of particle arrangement on soil functionality [11,15].

Since soil functionality depends on pore connectivity, porosity separation by volume is an important strategy used in tomography tests [72]. Pore branching and connectivity increase with pore volume. Based on this assumption, we defined connected soil porosity (Cp) as all pores exceeding 1-mm^3 volume. Our study reveals a more continuous pore system in topsoil, with Cp reducing with soil depth and varying little among cropping systems. Root development in topsoil and crop residue cycling are important factors in soil structuring and pore connectivity [45,73]. Soil disturbance can also generate large pores through decompaction and organic material incorporation [70]; however, these pores are predominantly discontinuous.

The connectivity index (Ci) expresses how much of the resolved porosity from CT analysis is connected porosity. Ci decreased with soil depth. The RFR-ct and RGrR-nt cropping systems had greater and similar Ci values in all layers, despite significant differences in management. Similar behavior in conventional tilled and grazed systems is unexpected, as plowing tends to break soil structure and disrupt porous space [18]. However, a large pore may not necessarily be continuous; it could be a hole or crack, commonly observed in soils tilled with agricultural machinery. The volume alone does not indicate connectivity.

The shape and complexity of pores indicate the porosity dynamics. Cropping systems in which soil is constantly tilled by plowing do not benefit soil structure due to the frequent aggregate breakdown and disruption of the pore network. Thus, soil under conventional tillage has many spherical, poorly branched pores that, even with a large volume, contribute little to flow dynamics within the soil [47]. Therefore, similar results may not indicate similar physical conditions, and CT allows for the visualization and determination of soil structural quality.

In addition to volume and shape, the probability of occurrence of connected pores in soil can be defined by the Γ indicator (global connectivity), another important parameter used in CT [41,42]. In agreement with the previously discussed parameters, the highest concentration of continuous pores occurs in topsoil. Grazed cropping systems can reduce continuous pores in deeper layers by obstructing pores via the root growth of summer crops and forage species [53,74]. Conversely, in conventional tillage (RFR-ct), residues are

fragmented and incorporated into deeper soil layers; consequently, the connected porosity of tilled soil is closely linked to the incorporated residues. Therefore, interconnected porosity is not necessarily the result of a complex process of soil structuring [75].

The CT analysis provided several parameters related to pore continuity and functionality. However, no significant correlation was observed between these parameters, contrary to many studies [8]. Nevertheless, most of these studies were conducted in highland soils with a strong structure [76,77]. In our study, image resolution (approximately 40 µm) allowed for the determination of macro- and mesopores. These pore classes are considered the most important for water and air movement in soil [16,78]. This indicates the distinct behavior of the clay-textured soil in our study.

Smaller-diameter pores (micropores) predominate in loam-textured soils [79] like the soil in this study. Furthermore, these soils exhibit lower aggregate stability, largely due to their sandy granulometry [80]. Soils with less aggregation usually have higher interconnected porosity, although they are more tortuous, and have more free space for flow [17,75]. In saturated soil, water flows through the entire pore space and is favored by large and continuous pores. Although loam texture soils facilitate water movement through smaller pores, this does not mean that cover crop management and conservation cropping systems do not improve structural quality. This soil requires management that provides the addition of organic matter and increases aggregate stability, with improvements in the porous system [81].

Soil K_a has a closer relationship with macroporosity, as the movement of gasses in soil depends on connected and drained pores [11,57]. For this reason, the no-tillage cropping systems with intense root production stood out with a reduction in soil water content, as these systems had long, continuous pores. Pore structure is quite complex, and the software was unable to differentiate a pore from a crack. Further, pore orientation is another major factor since a connected pore can be transverse to flow, thereby increasing the flow path. Therefore, 3D images are useful for assessing such differences and establishing relationships with soil functionality.

4.3. Qualitative Image Analysis

Several complexities can be only perceived when images are analyzed qualitatively. In Figure 6, images extracted from topsoil for Grazing 2019 are displayed (six years and six months after the experiment implementation), where a greater effect of management was expected. Differences in porosity structure are noticeable. The cropping system with inversion tillage (Figure 6A), as previously mentioned, has large, poorly connected pores, such as cavities related to tillage [73].

Grazed cropping systems have connected porosity linked to root growth and decomposition. The P4R-nt (Figure 6D) was the most distinguished grazed system, showing connected pores with greater diameter possibly due to biological activity and absence of soil tillage. A large volume of transversely arranged pores in topsoil results from intense animal trampling, as soils with sandy topsoil have low shear strength. Transversely arranged pores are not pedogenic pores but rather cracks that hardly fulfill the environmental function of structured pores formed by biological processes. Furthermore, transverse cracks are as harmful to water and air flow as soil compaction itself, by interrupting pore continuity [49]; therefore, K_a for this cropping system was close to the values for tilled soil.

The RGrR-nt and RGrS/RGrR-nt (Figures 6B and 6C, respectively) have an even more subtle difference, namely that both have fine, abundant pores. However, RGrR-nt has longer, straighter pores connecting extremities in the sample. As mentioned above, the orientation of the pore network plays an important role in pore functionality [11]. In contrast, the RGrS/RGrR-nt has more tortuous pores and, similarly to P4R-nt, has a higher concentration of transverse pores in topsoil, showing a negative effect of animal trampling and a greater susceptibility to compaction in this cropping system. The RGrR-nt benefits from the intense development of grasses both in summer and winter, protecting the soil

from harmful effects of trampling, and improving porosity structure by fine penetrating roots, which positively influence fluid flows in soil, mainly for air [23,55].

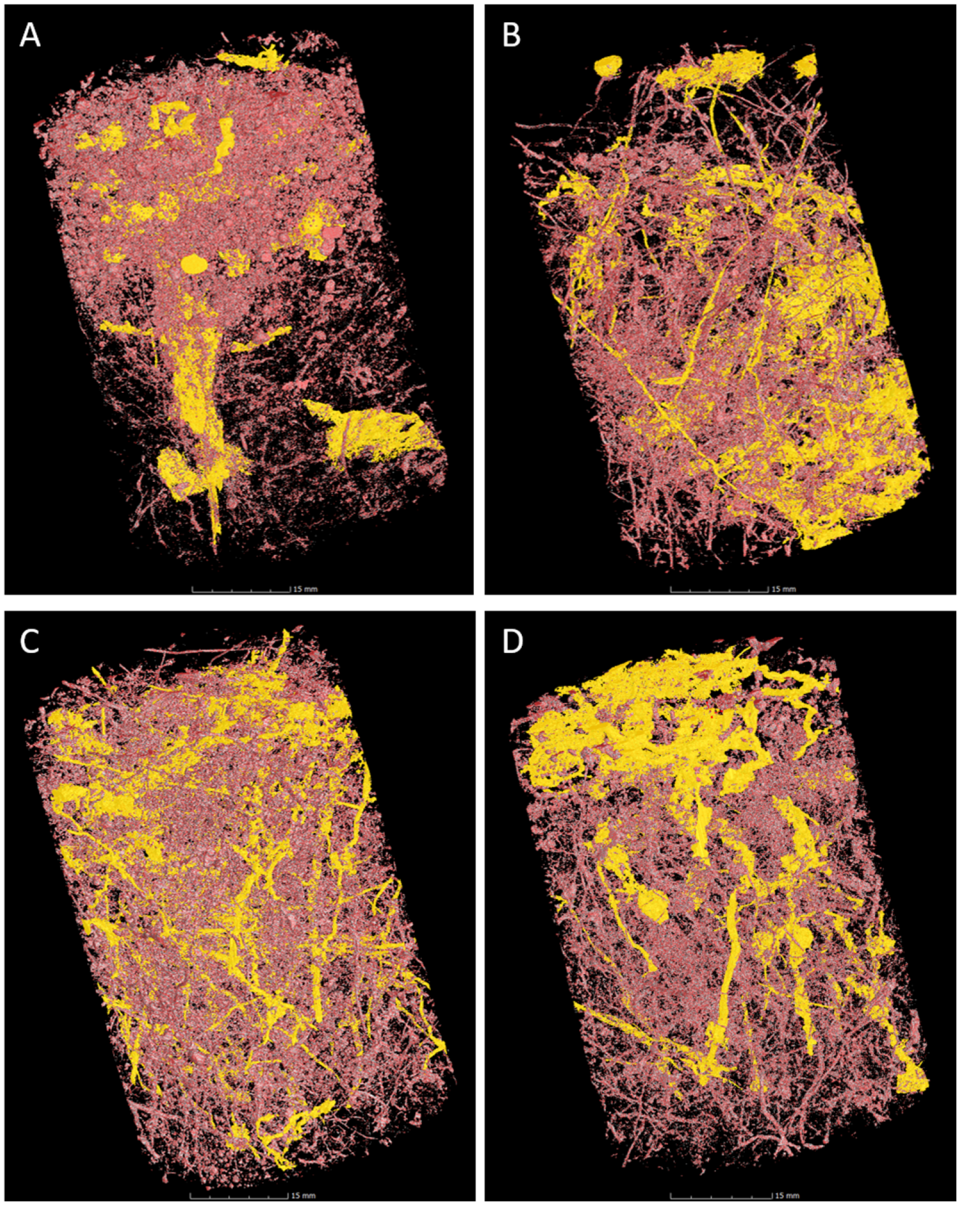

Figure 6. Three-dimensional image of total pores, with a volume > 10 mm^3 in yellow pores. (**A**) RFR-ct, (**B**) RGrR-nt, (**C**) RGrS/RGrR-nt, (**D**) P4R-nt, in a layer 0.0–0.06 m, for Grazing 2019. The samples are approximately 50 mm in diameter and 60 mm in height.

After relatively few years of implementing integrated crop–livestock systems in lowlands, differences in soil pore structure were already evident among the different managements. However, no significant effects on soil flow properties were observed. Therefore, it is still necessary to evaluate the soil structure after more rotation cycles for a better understanding of the long-term impacts of integrated crop–livestock systems on the dynamics between the soil's porous system and air and water flow processes in lowlands.

5. Conclusions

In lowlands, the semi-direct system with soil tillage did not differ from the cropping systems with livestock grazing regarding air and water flow through the soil. Soil tillage did not improve water and air permeability, and thus tillage is not required to reduce

soil compaction and enhance pore functioning. However, different grazing and soil cover configurations affect the soil structure and functionality.

Integrated agricultural cropping systems with a predominance of grasses (rice–ryegrass) improve soil structure, and mitigate the harmful effects of trampling, by increasing pore connectivity and functionality. Cropping systems with soybean cultivation or continuous grazing in winter and summer were detrimental to soil porosity, reducing soil permeability.

Pore connectivity parameters generated by X-ray computer tomography were less efficient for comparing cropping systems, mainly because tillage and organic material incorporation in semi-direct tillage increase pore volume and connectivity. A qualitative assessment of three-dimensional images revealed soil disturbance creates rounded, less continuous pores. For pore connectivity to express functionality, pores must be connected and continuous.

Grazed cropping systems with intense biological activity formed connected, elongated, continuous pores. A pore orientation positioned longitudinally to the flow increased soil capacity to conduct air. Nonetheless, continued grazing or reduced surface cover can disrupt pore continuity due to surface shearing by animal trampling.

Author Contributions: Conceptualization, J.V.A. and J.M.R.; Analysis, J.V.A. and D.L.S.; data curation, J.V.A.; writing—original draft preparation, J.V.A.; writing—review and editing, J.V.A., A.R.A., A.C.D.A. and J.M.R.; supervision, J.M.R.; funding acquisition, J.M.R. All authors have read and agreed to the published version of the manuscript.

Funding: This research was funded by Capes (Brazilian Federal Agency for Support and Evaluation of Graduate Education)—Finance code 001; RITES-FAPERGS Low Carbon Agriculture Adapted to Climate Changes in Rio Grande do Sul project (22/2551-0000392-3); CNPq-INCT Low Carbon Agriculture Project (406635/2022-6) and FINEP (Research and Projects Financing).

Institutional Review Board Statement: Not applicable.

Informed Consent Statement: Not applicable.

Data Availability Statement: The raw data will be made available by the authors on request.

Acknowledgments: The authors thank the research funding agencies for providing financial resources for the acquisition of the Nikon tomograph. We also thank P.C.F. Carvalho, from UFRGS, for allowing sample collection in his long-term field experiment.

Conflicts of Interest: The authors declare no conflicts of interest. The funders had no role in the design of the study; in the collection, analyses, or interpretation of data; in the writing of the manuscript; or in the decision to publish the results.

References

1. Sarkar, D.; Kar, S.K.; Chattopadhyay, A.; Shikha, R.A.; Tripathi, V.K.; Dubey, P.K.; Abhilash, P.C. Low input sustainable agriculture: A viable climate-smart option for boosting food production in a warming world. *Ecol. Indic.* **2020**, *115*, 106412. [CrossRef]
2. Sneessens, I.; Sauvée, L.; Randrianasolo-Rakotobe, H.; Ingrand, S. A framework to assess the economic vulnerability of farming systems: Application to mixed crop-livestock systems. *Agric. Syst.* **2019**, *176*, 102658. [CrossRef]
3. Sadowski, A.; Baer-Nawrocka, A. Food and environmental function in world agriculture—Interdependence or competition? *Land Use Policy* **2018**, *71*, 578–583. [CrossRef]
4. De Moraes, A.; Carvalho, P.C.D.F.; Anghinoni, I.; Lustosa, S.B.C.; Costa, S.E.V.G.A.; Kunrath, T.R. Integrated crop-livestock systems in the Brazilian subtropics. *Eur. J. Agron.* **2014**, *57*, 4–9. [CrossRef]
5. SOSBAI—Sociedade Sul-Brasileira de Arroz Irrigado. *Recomendações Técnicas da Pesquisa Para o Sul do Brasil*, 33rd ed.; SOSBAI: Restinga Seca, Brazil, 2022; p. 200.
6. Theisen, G.; Silva, J.J.C.; Silva, J.S.; Andres, A.; Anten, N.P.R.; Bastiaans, L. The birth of a new cropping system: Towards sustainability in the sub-tropical lowland agriculture. *Field Crops Res.* **2017**, *212*, 82–94. [CrossRef]
7. Rabot, E.; Wiesmeier, M.; Schlüter, S.; Vogel, H.J. Soil structure as an indicator of soil functions: A review. *Geoderma* **2018**, *314*, 122–137. [CrossRef]
8. Schlüter, S.; Sammartino, S.; Koestel, J. Exploring the relationship between soil structure and soil functions via pore-scale imaging. *Geoderma* **2020**, *370*, 114370. [CrossRef]
9. Reichert, J.M.; Mentges, M.I.; Rodrigues, M.F.; Cavalli, J.P.; Awe, G.O.; Mentges, L.R. Compressibility and elasticity of subtropical no-till soils varying in granulometry organic matter, bulk density and moisture. *Catena* **2018**, *165*, 345–357. [CrossRef]

10. Ambus, J.V.; Reichert, J.M.; Gubiani, P.I.; de Faccio Carvalho, P.C. Changes in composition and functional soil properties in long-term no-till integrated crop-livestock system. *Geoderma* **2018**, *330*, 232–243. [CrossRef]
11. Zhang, Z.; Liu, K.; Zhou, H.; Lin, H.; Li, D.; Peng, X. Linking saturated hydraulic conductivity and air permeability to the characteristics of biopores derived from X-ray computed tomography. *J. Hydrol.* **2019**, *571*, 1–10. [CrossRef]
12. Mentges, M.I.; Reichert, J.M.; Rodrigues, M.F.; Awe, G.O.; Mentges, L.R. Capacity and intensity soil aeration properties affected by granulometry, moisture, and structure in no-tillage soils. *Geoderma* **2016**, *263*, 47–59. [CrossRef]
13. Taiz, L.; Zeiger, E.; Moller, I.M.; Murphy, A. *Plant Physiology and Development*, 6th ed.; Sinauer Associates: Sunderland, MA, USA, 2014.
14. Vogeler, I.; Carrick, S.; Cichota, R.; Lilburne, L. Estimation of soil subsurface hydraulic conductivity based on inverse modelling and soil morphology. *J. Hydrol.* **2019**, *574*, 373–382. [CrossRef]
15. Feng, Y.; Wang, J.; Liu, T.; Bai, Z.; Reading, L. Using computed tomography images to characterize the effects of soil compaction resulting from large machinery on three-dimensional pore characteristics in an opencast coal mine dump. *J. Soils Sediments* **2019**, *19*, 1467–1478. [CrossRef]
16. Borges, J.A.R.; Pires, L.F.; Cássaro, F.A.M.; Auler, A.C.; Rosa, J.A.; Heck, R.J.; Roque, W.L. X-ray computed tomography for assessing the effect of tillage systems on topsoil morphological attributes. *Soil Tillage Res.* **2019**, *189*, 25–35. [CrossRef]
17. Pires, L.F.; Borges, J.A.R.; Rosa, J.A.; Cooper, M.; Heck, R.J.; Passoni, S.; Roque, W.L. Soil structure changes induced by tillage systems. *Soil Tillage Res.* **2017**, *165*, 66–79. [CrossRef]
18. Eze, S.; Dougill, A.J.; Banwart, S.A.; Hermans, T.D.G.; Ligowe, I.S.; Thierfelder, C. Impacts of conservation agriculture on soil structure and hydraulic properties of Malawian agricultural systems. *Soil Tillage Res.* **2020**, *201*, 104639. [CrossRef]
19. Kunz, M.; Gonçalves, A.D.M.D.A.; Reichert, J.M.; Guimarães, R.M.L.; Reinert, D.J.; Rodrigues, M.F. Compactação do solo na integração soja-pecuária de leite em Latossolo argiloso com semeadura direta e escarificação. *Rev. Bras. Cienc. Solo* **2013**, *37*, 1699–1708. [CrossRef]
20. Negrón, M.; López, I.; Dörner, J. Consequences of intensive grazing by dairy cows of contrasting live weights on volcanic ash topsoil structure and pasture dynamics. *Soil Tillage Res.* **2019**, *189*, 88–97. [CrossRef]
21. Lucas, M.; Schlüter, S.; Vogel, H.J.; Vetterlein, D. Soil structure formation along an agricultural chronosequence. *Geoderma* **2019**, *350*, 61–72. [CrossRef]
22. Adetunji, A.T.; Ncube, B.; Mulidzi, R.; Lewu, F.B. Management impact and benefit of cover crops on soil quality: A review. *Soil Tillage Res.* **2020**, *204*, 104717. [CrossRef]
23. Lu, J.; Zhang, Q.; Werner, A.D.; Li, Y.; Jiang, S.; Tan, Z. Root-induced changes of soil hydraulic properties—A review. *J. Hydrol.* **2020**, *589*, 125203. [CrossRef]
24. Nunes, M.R.; Karlen, D.L.; Veum, K.S.; Moorman, T.B.; Cambardella, C.A. Biological soil health indicators respond to tillage intensity: A US meta-analysis. *Geoderma* **2020**, *369*, 114335. [CrossRef]
25. Villarreal, R.; Lozano, L.A.; Salazar, M.P.; Bellora, G.L.; Melani, E.M.; Polich, N.; Soracco, C.G. Pore system configuration and hydraulic properties. Temporal variation during the crop cycle in different soil types of Argentinean Pampas Region. *Soil Tillage Res.* **2020**, *198*, 104528. [CrossRef]
26. Assmann, J.M.; Anghinoni, I.; Martins, A.P.; de Andrade, S.E.V.G.; Cecagno, D.; Carlos, F.S.; de Faccio Carvalho, P.C. Soil carbon and nitrogen stocks and fractions in a long-term integrated crop–livestock system under no-tillage in southern Brazil. *Agric. Ecosyst. Environ.* **2014**, *190*, 52–59. [CrossRef]
27. Kottek, M.; Grieser, J.; Beck, C.; Rudolf, B.; Rubel, F. World map of the Köppen-Geiger climate classification updated. *Meteorolo. Z.* **2006**, *15*, 259–263. [CrossRef]
28. USDA. *Keys to Soil Taxonomy*, 14th ed.; United States Department of Agriculture—USDA: Washington, WA, USA, 2014; p. 372.
29. Santos, H.G.; Jacomine, P.K.T.; Anjos, L.H.C.; Oliveira, V.A.; Lumbreras, J.F.; Coelho, M.R.; Almeida, J.A.; Araújo Filho, J.C.; Oliveira, J.B.; Cunha, T.J.F. *Sistema Brasileiro de Classificação de Solos*, 5th ed.; Embrapa Solos: Rio de Janeiro, Brazil; Embrapa: Brasilia, Brazil, 2018; p. 353.
30. Carmona, F.C.; Denardin, L.G.O.; Martins, A.P.; Anghinoni, I.; Carvalho, P.C.F. *Sistemas Integrados de Produção Agropecuária em Terras Baixas*; Gráfica e Editora RJR: Porto Alegre, Brazil, 2018; p. 160.
31. Dominschek, R.; Schuster, M.Z.; Barroso, A.A.M.; Moraes, A.; Anghinoni, I.; Carvalho, P.C.F. Diversification of traditional paddy field impacts target species in weed seedbank. *Rev. Cien. Agron.* **2022**, *53*, e20207471. [CrossRef]
32. Gubiani, P.I.; Albuquerque, J.A.; Reinert, D.J.; Reichert, J.M. Tensão e extração de água em mesa de tensão e coluna de areia, em dois solos com elevada densidade. *Cienc. Rural* **2009**, *39*, 2535–2538. [CrossRef]
33. Horn, R.; Vossbrink, J.; Becker, S. Modern forestry vehicles and their impacts on soil physical properties. *Soil Tillage. Res.* **2004**, *79*, 207–219. [CrossRef]
34. Libardi, P.L. *Dinâmica Da Da Água No Solo*; Ed USP: São Paulo, Brazil, 2005; p. 331.
35. Anderson, S.H.; Gantzer, C.J.; Boone, J.M.; Tully, R.J. Rapid Nondestructive Bulk Density and Soil-Water Content Determination by Computed Tomography. *Soil Sci. Soc. Am. J.* **1988**, *52*, 35–40. [CrossRef]
36. Sleutel, S.; Cnudde, V.; Masschaele, B.; Vlassenbroek, J.; Dierick, M.; Van Hoorebeke, L.; Jacobs, P.; De Neve, S. Comparison of different nano- and micro-focus X-ray computed tomography set-ups for the visualization of the soil microstructure and soil organic matter. *Comput. Geosci.* **2008**, *34*, 931–938. [CrossRef]

37. Van Loo, D.; Bouckaert, L.; Leroux, O.; Pauwels, E.; Dierick, M.; Van Hoorebeke, L.; Cnudde, V.; De Neve, S.; Sleutel, S. Contrast agents for soil investigation with X-ray computed tomography. *Geoderma* **2014**, *213*, 485–491. [CrossRef]
38. Kuka, K.; Illerhaus, B.; Fox, C.A.; Joschko, M. X-ray Computed Microtomography for the Study of the Soil–Root Relationship in Grassland Soils. *Vadose Z. J.* **2013**, *12*, 1–10. [CrossRef]
39. Scheffer, K.; Méheust, Y.; Carvalho, M.S.; Mauricio, M.H.P.; Paciornik, S. Enhancement of oil recovery by emulsion injection: A pore scale analysis from X-ray micro-tomography measurements. *J. Pet. Sci. Eng.* **2021**, *198*, 108134. [CrossRef]
40. Pfeifer, J.; Kirchgessner, N.; Colombi, T.; Walter, A. Rapid phenotyping of crop root systems in undisturbed field soils using X-ray computed tomography. *Plant Methods* **2015**, *11*, 41. [CrossRef]
41. Lucas, M.; Vetterlein, D.; Vogel, H.J.; Schlüter, S. Revealing pore connectivity across scales and resolutions with X-ray CT. *Eur. J. Soil Sci.* **2021**, *72*, 546–560. [CrossRef]
42. Renard, P.; Allard, D. Connectivity metrics for subsurface flow and transport. *Adv. Water Resour.* **2013**, *51*, 168–196. [CrossRef]
43. R Core Team. *R: A Language and Environment for Statistical Computing*; R Foundation for Statistical Computing: Vienna, Austria, 2023. Available online: https://www.R-project.org/ (accessed on 1 May 2024).
44. de Andrade Bonetti, J.; Anghinoni, I.; Ivonir Gubiani, P.; Cecagno, D.; de Moraes, M.T. Impact of a long-term crop-livestock system on the physical and hydraulic properties of an Oxisol. *Soil Tillage Res.* **2019**, *186*, 280–291. [CrossRef]
45. Patra, S.; Julich, S.; Feger, K.H.; Jat, M.L.; Jat, H.; Sharma, P.C.; Schwärzel, K. Soil hydraulic response to conservation agriculture under irrigated intensive cereal-based cropping systems in a semiarid climate. *Soil Tillage Res.* **2019**, *192*, 151–163. [CrossRef]
46. Kreiselmeier, J.; Chandrasekhar, P.; Weninger, T.; Schwen, A.; Julich, S.; Feger, K.H.; Schwärzel, K. Temporal variations of the hydraulic conductivity characteristic under conventional and conservation tillage. *Geoderma* **2020**, *362*, 114127. [CrossRef]
47. Ambus, J.V.; Awe, G.O.; Faccio Carvalho PC de Reichert, J.M. Integrated crop-livestock systems in lowlands with rice cultivation improve root environment and maintain soil structure and functioning. *Soil Tillage Res.* **2023**, *227*, 105592. [CrossRef]
48. Vanderburg, K.L.; Steffens, T.J.; Lust, D.G.; Rhoades, M.B.; Blaser, B.C.; Peters, K.; Ham, M.J. Trampling and Cover Effects on Soil Compaction and Seedling Establishment in Reseeded Pasturelands Over Time. *Rangel Ecol. Manag.* **2020**, *73*, 452–461. [CrossRef]
49. Berisso, F.E.; Schjønning, P.; Lamandé, M.; Weisskopf, P.; Stettler, M.; Keller, T. Effects of the stress field induced by a running tyre on the soil pore system. *Soil Tillage Res.* **2013**, *131*, 36–46. [CrossRef]
50. Gubiani, P.I.; Müller, E.A.; Somavilla, A.; Zwirtes, A.L.; Mulazzani, R.P.; Marchesan, E. Transpiration reduction factor and soybean yield in low land soil with ridge and chiseling. *Rev. Bras. Cienc. Solo* **2018**, *42*, e0170282. [CrossRef]
51. Gregorutti, V.C.; Caviglia, O.P. Impact of crop aerial and root biomass inputs on soil nitrifiers and cellulolytic microorganisms. *Soil Tillage Res.* **2019**, *191*, 85–97. [CrossRef]
52. Silva MF da Fernandes, M.M.H.; Fernandes, C.; Silva AMR da Ferraudo, A.S.; Coelho, A.P. Contribution of tillage systems and crop succession to soil structuring. *Soil Tillage Res.* **2021**, *209*, 104924. [CrossRef]
53. Nguyen, B.T.; Ishikawa, T.; Murakami, T. Effects evaluation of grass age on hydraulic properties of coarse-grained soil. *Transp. Geotech.* **2020**, *25*, 100401. [CrossRef]
54. Pöhlitz, J.; Rücknagel, J.; Schlüter, S.; Vogel, H.J.; Christen, O. Estimation of critical stress ranges to preserve soil functions for differently textured soils. *Soil Tillage Res.* **2020**, *200*, 104637. [CrossRef]
55. Hao, H.X.; Wei, Y.J.; Cao, D.N.; Guo, Z.L.; Shi, Z.H. Vegetation restoration and fine roots promote soil infiltrability in heavy-textured soils. *Soil Tillage Res.* **2020**, *198*, 104542. [CrossRef]
56. Martínez, I.; Chervet, A.; Weisskopf, P.; Sturny, W.G.; Rek, J.; Keller, T. Two decades of no-till in the Oberacker long-term field experiment: Part II. Soil porosity and gas transport parameters. *Soil Tillage Res.* **2016**, *163*, 130–140. [CrossRef]
57. Holthusen, D.; Brandt, A.A.; Reichert, J.M.; Horn, R. Soil porosity, permeability and static and dynamic strength parameters under native forest/grassland compared to no-tillage cropping. *Soil Tillage Res.* **2018**, *177*, 113–124. [CrossRef]
58. Turek, M.E.; de Jong van Lier, Q.; Armindo, R.A. Estimation and mapping of field capacity in Brazilian soils. *Geoderma* **2020**, *376*, 114557. [CrossRef]
59. Parfitt, J.M.B.; Concenço, G.; Scivittaro, W.B.; Andres, A.; da Silva, J.T.; Pinto, M.A.B. Soil and Water Management for Sprinkler Irrigated Rice in Southern Brazil. In *Advances in International Rice Research*; IntechOpen: Rijeka, Croatia, 2017; pp. 3–18. [CrossRef]
60. de Faccio Carvalho, P.C.; Anghinoni, I.; de Moraes, A.; de Souza, E.D.; Sulc, R.M.; Lang, C.R.; Flores, J.P.C.; Terra Lopes, M.L.; da Silva, J.L.S.; Conte, O.; et al. Managing grazing animals to achieve nutrient cycling and soil improvement in no-till integrated systems. *Nutr. Cycl. Agroecosyst.* **2010**, *88*, 259–273. [CrossRef]
61. Reichert, J.M.; Brandt, A.A.; Rodrigues, M.F.; Reinert, D.J.; Braida, J.A. Load dissipation by corn residue on tilled soil in laboratory and field-wheeling conditions. *J. Sci. Food Agric.* **2016**, *96*, 2705–2714. [CrossRef] [PubMed]
62. Baggio, C.; Carvalho, P.C.D.F.; Silva, J.L.S.D.; Anghinoni, I.; Lopes, M.L.T.; Thurow, J.M. Padrões de deslocamento e captura de forragem por novilhos em pastagem de azevém-anual e aveia-preta manejada sob diferentes alturas em sistema de integração lavoura-pecuária. *Rev. Bras. Zootec.* **2009**, *38*, 215–222. [CrossRef]
63. Liu, Y.; Cui, Z.; Huang, Z.; López-Vicente, M.; Wu, G.L. Influence of soil moisture and plant roots on the soil infiltration capacity at different stages in arid grasslands of China. *Catena* **2019**, *182*, 104147. [CrossRef]
64. Shen, X.; Yang, F.; Xiao, C.; Zhou, Y. Increased contribution of root exudates to soil carbon input during grassland degradation. *Soil Biol. Biochem.* **2020**, *146*, 107817. [CrossRef]

65. Wahlström, E.M.; Kristensen, H.L.; Thomsen, I.K.; Labouriau, R.; Pulido-Moncada, M.; Nielsen, J.A.; Munkholm, L.J. Subsoil compaction effect on spatio-temporal root growth, reuse of biopores and crop yield of spring barley. *Eur. J. Agron.* **2021**, *123*, 126225. [CrossRef]
66. Holthusen, D.; Brandt, A.A.; Reichert, J.M.; Horn, R.; Fleige, H.; Zink, A. Soil functions and in situ stress distribution in subtropical soils as affected by land use, vehicle type, tire inflation pressure and plant residue removal. *Soil Tillage Res.* **2018**, *184*, 78–92. [CrossRef]
67. Naveed, M.; Schjønning, P.; Keller, T.; de Jonge, L.W.; Moldrup, P.; Lamandé, M. Quantifying vertical stress transmission and compaction-induced soil structure using sensor mat and X-ray computed tomography. *Soil Tillage Res.* **2016**, *158*, 110–122. [CrossRef]
68. Braida, J.A.; Reichert, J.M.; Reinert, D.J.; Sequinatto, L. Soil elasticity as affected by water and organic carbon content. *Rev. Bras. Cienc. Solo* **2008**, *32*, 477–485. [CrossRef]
69. Awe, G.O.; Reichert, J.M.; Holthusen, D.; Ambus, J.V.; de Faccio Carvalho, P.C. Characterization of microstructural stability of biochar-amended Planosol under conventional tillage for irrigated lowland rice ecosystem. *Soil Tillage Res.* **2021**, *212*, 105051. [CrossRef]
70. Schlüter, S.; Großmann, C.; Diel, J.; Wu, G.M.; Tischer, S.; Deubel, A.; Rücknagel, J. Long-term effects of conventional and reduced tillage on soil structure, soil ecological and soil hydraulic properties. *Geoderma* **2018**, *332*, 10–19. [CrossRef]
71. Mondal, S.; Chakraborty, D.; Das, T.K.; Shrivastava, M.; Mishra, A.K.; Bandyopadhyay, K.K.; Aggarwal, P.; Chaudhari, S.K. Conservation agriculture had a strong impact on the sub-surface soil strength and root growth in wheat after a 7-year transition period. *Soil Tillage Res.* **2019**, *195*, 104385. [CrossRef]
72. Zhao, Y.; Hu, X.; Li, X. Analysis of the intra-aggregate pore structures in three soil types using X-ray computed tomography. *Catena* **2020**, *193*, 104622. [CrossRef]
73. Soto-Gómez, D.; Pérez-Rodríguez, P.; Vázquez-Juiz, L.; López-Periago, J.E.; Paradelo, M. Linking pore network characteristics extracted from CT images to the transport of solute and colloid tracers in soils under different tillage managements. *Soil Tillage Res.* **2018**, *177*, 145–154. [CrossRef]
74. Ni, J.J.; Ng, C.W.W. Long-term effects of grass roots on gas permeability in unsaturated simulated landfill covers. *Sci. Total Environ.* **2019**, *666*, 680–684. [CrossRef]
75. dos Reis, A.M.H.; Auler, A.C.; Armindo, R.A.; Cooper, M.; Pires, L.F. Micromorphological analysis of soil porosity under integrated crop-livestock management systems. *Soil Tillage Res.* **2021**, *205*, 104783. [CrossRef]
76. Schlüter, S.; Albrecht, L.; Schwärzel, K.; Kreiselmeier, J. Long-term effects of conventional tillage and no-tillage on saturated and near-saturated hydraulic conductivity—Can their prediction be improved by pore metrics obtained with X-ray CT? *Geoderma* **2020**, *361*, 114082. [CrossRef]
77. Piccoli, I.; Schjønning, P.; Lamandé, M.; Zanini, F.; Morari, F. Coupling gas transport measurements and X-ray tomography scans for multiscale analysis in silty soils. *Geoderma* **2019**, *338*, 576–584. [CrossRef]
78. Katuwal, S.; Norgaard, T.; Moldrup, P.; Lamandé, M.; Wildenschild, D.; de Jonge, L.W. Linking air and water transport in intact soils to macropore characteristics inferred from X-ray computed tomography. *Geoderma* **2015**, *238*, 9–20. [CrossRef]
79. da Silva, L.F.; Fruett, T.; Zinn, Y.L.; Inda, A.V.; do Nascimento, P.C. Genesis, morphology and mineralogy of Planosols developed from different parent materials in southern Brazil. *Geoderma* **2019**, *341*, 46–58. [CrossRef]
80. Ge, N.; Wei, X.; Wang, X.; Liu, X.; Shao, M.; Jia, X.; Li, X.; Zhang, Q. Soil texture determines the distribution of aggregate-associated carbon, nitrogen and phosphorous under two contrasting land use types in the Loess Plateau. *Catena* **2019**, *172*, 148–157. [CrossRef]
81. Menon, M.; Mawodza, T.; Rabbani, A.; Blaud, A.; Lair, G.J.; Babaei, M.; Kercheva, M.; Rousseva, S.; Banwart, S. Pore system characteristics of soil aggregates and their relevance to aggregate stability. *Geoderma* **2020**, *366*, 114259. [CrossRef]